

나노입자가 포함된 촉진수송 분리막에서의 메조기공 티타늄산화물의 영향

김 상 진 · 정 정 표 · 김 동 준 · 김 중 학[†]

연세대학교 화공생명공학과
(2015년 10월 7일 접수, 2015년 10월 21일 수정, 2015년 10월 21일 채택)

Effect of Mesoporous TiO₂ in Facilitated Olefin Transport Membranes Containing Ag Nanoparticles

Sang Jin Kim, Jung Pyu Jung, Dong Jun Kim, and Jong Hak Kim[†]

Department of Chemical and Biomolecular Engineering, Yonsei University, 50 Yonsei-ro, Seodaemun-gu, Seoul 03722, Korea
(Received October 7, 2015, Revised October 21, 2015, Accepted October 21, 2015)

요 약: 용액-확산 메커니즘에 의해 결정되는 기존의 고분자에서와는 달리, 촉진수송은 투과도와 선택도를 동시에 향상시킬 수 있는 기술이다. 본 연구에서는 은 나노입자, 폴리비닐피롤리돈, 7,7,8,8-테트라시아노퀴노디메탄으로 구성된 촉진수송 올레핀 분리막에 있어서, 메조기공 티타늄산화물(m-TiO₂)에 대한 영향을 연구하였다. 특히 메조기공 티타늄산화물은 폴리비닐클로라이드-g-폴리옥시에틸렌 메타크릴레이트 가지형 공중합체를 템플레이트로 하여 쉽고 대량 생산이 가능한 방법으로 제조하였다. 엑스레이 회절분석에 따르면, 제조된 메조기공 티타늄산화물은 아나타제와 루타일 상의 혼합으로 구성되어 있으며, 결정의 크기가 약 16 nm 정도 되었다. 메조기공 티타늄산화물을 첨가하였을 때, 분리막의 확산도가 증가하여 혼합기체 투과도가 1.6에서 16 GPU로 증가하였고 선택도는 45에서 37로 약간 감소하였다. 메조기공 티타늄산화물이 첨가되지 않은 분리막은 장시간 성능이 유지되었으나, 메조기공 티타늄산화물이 첨가된 분리막의 경우 시간이 지남에 따라 투과도와 선택도가 감소하였다. 이는 티타늄산화물과 은 사이의 화학적 상호작용으로 은 나노입자의 올레핀 운반체로서의 활성을 감소시키기 때문으로 사료된다.

Abstract: Facilitated transport is considered to be a possible solution to simultaneously improve permeability and selectivity, which is challenging in normal polymeric membranes based on solution-diffusion transport only. We investigated the effect of adding mesoporous TiO₂ (m-TiO₂) upon the separation performance of facilitated olefin transport membranes comprising poly(vinyl pyrrolidone), Ag nanoparticles, and 7,7,8,8-tetracyanoquinodimethane as the polymer matrix, olefin carrier, and electron acceptor, respectively. In particular, m-TiO₂ was prepared by means of a facile, mass-producible method using poly(vinyl chloride)-g-poly(oxyethylene methacrylate) graft copolymer as the template. The crystal phase of m-TiO₂ consisted of an anatase/rutile mixture, of crystallite size approximately 16 nm as determined by X-ray diffraction. The introduction of m-TiO₂ increased the membrane diffusivity, thereby increasing the mixed-gas permeance from 1.6 to 16.0 GPU (1 GPU = 10⁻⁶ cm³(STP)/(s × cm² × cmHg), and slightly decreased the propylene/propane selectivity from 45 to 37. However, both the mixed-gas permeance and selectivity of the membrane containing m-TiO₂ rapidly decreased over time, whereas the membrane without m-TiO₂ had more stable long-term performance. This difference might be attributed to specific chemical interactions between TiO₂ and Ag nanoparticles, causing Ag to lose activity as an olefin carrier.

Keywords: facilitated transport, silver nanoparticle, TiO₂, olefin carrier, electron acceptor

1. Introduction

Nanomaterials such as nanoparticles, nanocomposites, and nanostructures have received much attention due to

their unique optical, electrical, mechanical, and transport properties[1-6]. These properties have enabled versatile applications in catalysis, drug delivery, sensors, and photonics[7-13]. Among them, metal nanoparticles

[†]Corresponding author(e-mail: jonghak@yonsei.ac.kr, <http://orcid.org/0000-0002-5858-1747>)

have been employed in gas separation membranes to form mixed matrix membranes[14-20]. Recently, a new approach to prepare facilitated olefin transport membranes has been suggested, based on the specific and reversible interaction between olefin molecules such as ethylene and propylene and metallic silver nanoparticles (AgNPs) with positive surface charge[21-23].

Facilitated transport is defined as the combined mass transport of solution-diffusion transport and of carrier-mediated transport arising from reversible reactions between the carrier in a membrane and a specific permeant. The carrier in the membrane is able to reversibly form a complex with a target permeant, thereby improving the mass transport rate and the membrane's permeability. Thus, facilitated transport is considered to be a possible solution to simultaneously improve permeability and selectivity, which is challenging in normal polymeric membranes based on solution-diffusion transport only[21-23].

Recently, Kang's group reported that positively charged AgNPs played a pivotal role as the olefin carrier, inducing facilitated olefin transport. For example, poly(ethylene-co-propylene)/AgNP/p-benzoquinone composite membranes have shown propylene/propane selectivity of 11 and total mixed-gas permeance of 0.5 gas permeation units (GPU; $1 \text{ GPU} = 10^{-6} \text{ cm}^3 \text{ (STP)} \text{ s}^{-1} \text{ cm}^{-2} \text{ cmHg}^{-1}$); these are both much higher than those of pristine poly(ethylene-co-propylene) membranes[21]. Later, significantly improved separation performance (selectivity of 50 and permeance of 3.5 GPU) was reported based on a composite consisting of poly(vinyl pyrrolidone) (PVP)/AgNP/7,7,8,8-tetracyanoquinodimethane (TCNQ), in which TCNQ functioned as a strong electron acceptor[22].

A mixed matrix membrane consists of an inorganic filler dispersed in a polymer matrix; the fillers used include metal-organic frameworks, zeolites, carbon nanotubes, or metal oxides[24-29]. Among the various filler materials, titanium dioxide (TiO_2) has attracted a good deal of attention due to its low cost and ease of preparation. For example, P25 (a trade name for a commercially available TiO_2 nanopowder) has been

used as a filler with glassy polymers such as polyimide or poly(1-trimethylsilyl-1-propyne) to form mixed matrix membranes[30-36]. However, there has been no report on the use of TiO_2 in AgNP-based facilitated transport membranes for olefin/paraffin separation.

Herein we report facilitated olefin transport membranes consisting of PVP, AgNPs, TCNQ, and mesoporous TiO_2 (m- TiO_2) as the polymer matrix, olefin carrier, electron acceptor, and transport channel medium, respectively. The m- TiO_2 filler was templated using an amphiphilic poly(vinyl chloride)-g-poly(oxyethylene methacrylate) (PVC-g-POEM) graft copolymer. The effect of m- TiO_2 filler content upon membrane performance, including mixed-gas permeance and propylene/propane selectivity, was investigated in detail.

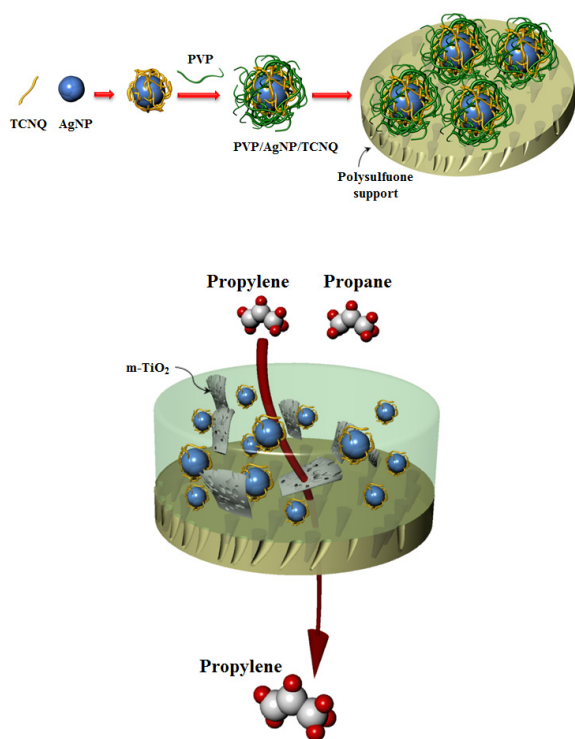
2. Experimental

2.1. Materials

Silver tetrafluoroborate (AgBF_4 , 98%) was purchased from TCI Fine Chemicals. Poly(vinyl pyrrolidone) (PVP, $M_w = 28,000\text{-}32,000 \text{ g/mol}$), 7,7,8,8-tetracyanoquinodimethane (TCNQ), poly(vinyl chloride) (PVC, $M_n = 99,000 \text{ g/mol}$), poly(oxyethylene methacrylate) (POEM, poly(ethylene glycol) methyl ether methacrylate, $M_n = 475 \text{ g/mol}$), 1,1,4,7,10,10-hexamethyltriethylene tetramine (HMTETA, 99%), copper (I) chloride (CuCl , 99%), and titanium isopropoxide (TTIP) were purchased from Aldrich. Tetrahydrofuran, *N*-methyl pyrrolidone, and methanol were obtained from J. T. Baker. All chemicals were of reagent grade and were used as received.

2.2. Synthesis of PVC-g-POEM

PVC-g-POEM graft copolymer was synthesized by means of a typical atom transfer radical polymerization (ATRP) procedure[37-40]. First, 3 g of PVC was dissolved in 50 ml of *N*-methyl pyrrolidone by stirring at room temperature for 1 d. Then, 0.05 g of CuCl was added, followed by 9 mL of POEM; subsequently, 0.12 mL of HMTETA was immediately added to the solution. The resulting green reaction solution was



Scheme 1. Schematic illustration of the formation of PVP/AgNP/TCNQ/m-TiO₂ composite membranes on a microporous polysulfone support.

purged with nitrogen for 30 min and then reacted at 90°C for 24 h. After polymerization, the completed reaction mixtures were precipitated into methanol three times. The reaction products were dried overnight in an oven at 50°C, and were then dried overnight in a vacuum oven at room temperature.

2.3. Synthesis of m-TiO₂

A TTIP sol-gel solution was prepared by adding 2 mL of hydrochloric acid (37%, HCl) dropwise into 4 mL of TTIP solution under vigorous stirring, followed by adding 2 mL of distilled water. This solution was stirred vigorously for an additional 30 min and mixed with a 10% solution of PVC-g-POEM in tetrahydrofuran. The resulting mixture was stirred for 1 day and then calcined at 450°C for 2 h[38,39].

2.4. Preparation of membranes

PVP/AgNP/TCNQ/m-TiO₂ composite membranes were prepared by dispersing TCNQ and m-TiO₂ into a 20

wt% solution of PVP-protected AgNPs in EtOH[23]. The weight ratio of PVP to AgNPs was fixed at 1/0.5. The mixed solution was then coated onto a porous polysulfone support (Toray Chemical Industries Inc.) using an RK Control Coater (Model 101, Control Coater RK Print-Coat Instruments Ltd., UK). The solvent was removed by evaporation in a convection oven at room temperature, followed by drying in a vacuum oven for 1 day.

2.5. Separation performance

The 50 : 50 propylene/propane mixed-gas separation properties of composite membranes (area 2.25 cm²) were evaluated by using a gas chromatograph (Young Lin 6500 GC system) equipped with a TCD detector and a column packed with Unibeads 2S 60/80. The gas flow rates were controlled using mass flow controllers. Gas permeance values were measured with an upstream flow meter with the feed pressure (4 atm) and atmospheric downstream pressure.

3. Results and discussion

PVP/AgNP/TCNQ/m-TiO₂ composite membranes were prepared in which AgNPs were activated by TCNQ (Scheme 1). The AgNPs have a specific interaction with TCNQ that generates an interfacial dipole on the Ag metal surface[41]. The AgNPs, stabilized and polarized by TCNQ, were well dispersed throughout the PVP matrix, and were then coated onto a microporous polysulfone support to form composite membranes. The additive m-TiO₂ is expected to play a role as a transport channel medium, increasing the membrane's diffusivity and permeability.

m-TiO₂ was prepared based on a PVC-g-POEM graft copolymer template via the sol-gel process, which is a facile, nonhydrothermal method. The morphology of the resulting m-TiO₂ is shown in Fig. 1. The m-TiO₂ particles were approximately 1-2 μm in size and had pores 30-50 nm in size. PVC-g-POEM worked as a structure-directing agent due to its amphiphilic, micro-phase-separated structure that transitions to a glassy, hydrophobic PVC main chain with rubbery, hydrophilic

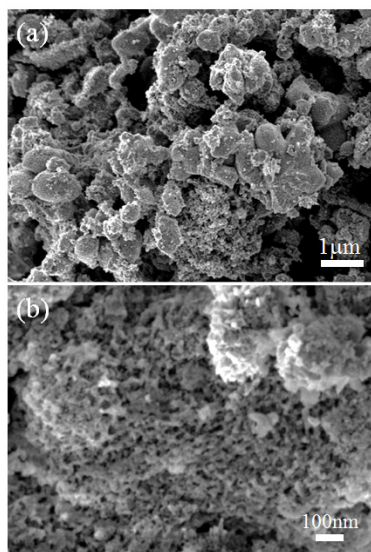


Fig. 1. SEM images of m-TiO₂ prepared by means of sol-gel reaction using a PVC-g-POEM graft copolymer.

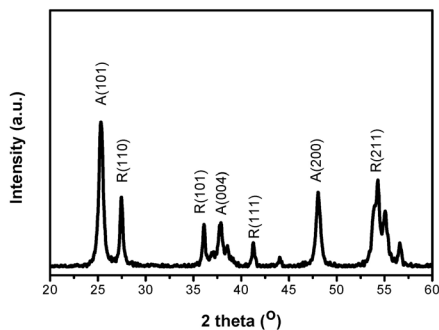


Fig. 2. XRD pattern of m-TiO₂ prepared by means of sol-gel reaction using a PVC-g-POEM graft copolymer.

POEM side chains[38,39]. The titania precursor (i.e. TTIP) was a small hydrophilic compound, and thus it strongly interacted with and was preferentially confined within the hydrophilic POEM domains. Upon calcination at 450°C for 2 h, the PVC-g-POEM graft copolymers burned out completely to generate mesopores while the m-TiO₂ proceeded to form by means of in situ crystallite formation. Because the hydrophobic PVC main chains have no specific interaction with hydrophilic TTIP, the pores were generated predominantly from the PVC main chains. The mesoporous structure of titania would help to facilitate gas transport and improve interfacial contact with the polymer matrix.

Table 1. Mixed-gas Permeances and Propylene/propane Selectivities of Various Membranes

Membrane	Permeance (GPU)	Selectivity (propylene/propane)
PVP/AgNP	0.8	1.1
PVP/AgNP/TCNQ	1.6	45
PVP/AgNP/TCNQ/m-TiO ₂ 10 wt% (10 min)	16.0	37
PVP/AgNP/TCNQ/m-TiO ₂ 10 wt% (3 h)	1.2	14

The crystalline structure of m-TiO₂ was characterized by XRD (Fig. 2). Several strong crystalline peaks were observed for m-TiO₂. Strong peaks at 2θ of 25.5, 38.0°, and 48.2° corresponded to the (101), (004), and (200) planes of the anatase TiO₂ phase, respectively (ICDD-JCPDS No.86-1157). Strong peaks observed at 2θ of 27.5, 36.2, 41.4°, and 54.5° were assigned to the (110), (101), (111), and (211) planes of the rutile TiO₂ phase, respectively (ICDD-JCPDS database, No. 77-0441). Thus, the crystal phases of m-TiO₂ comprised a mixture of anatase/rutile TiO₂, though anatase was the primary component. The average crystallite size (t) was calculated using Bragg's equation, where k is the shape factor of the particle (0.89), λ is the wavelength of the X-ray source (λ = 1.5406 Å), B is the full width at half maximum (FWHM) of the (101) diffraction peak, and θ is half of Bragg's diffraction angle of the centroid of the peak, in degrees; $t = \frac{\kappa\lambda}{B \cos \theta}$. The m-TiO₂ crystallite size was thus determined to be approximately 16 nm. The mesoporous structure could be attributed to the effective role of the PVC-g-POEM graft copolymer as a template.

First, to investigate the effect of using TCNQ on the resulting propylene/propane separation performance, AgNPs were generated utilizing AgBF₄ as a precursor in the PVP matrix, without the use of TCNQ. As shown in Table 1, the resulting PVP/AgNP composite membrane showed a propylene/propane selectivity of 1.1 and a mixed-gas permeance of 0.8 GPU. The reason for this poor selectivity is that the AgNPs in the

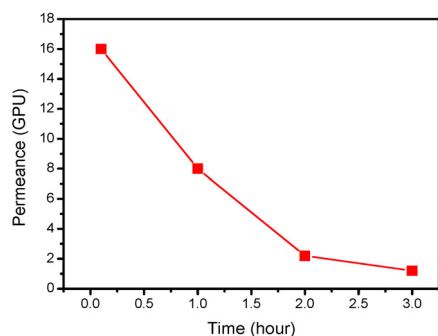


Fig. 3. Mixed-gas permeance versus time of PVP/AgNP/TCNQ membranes with 10 wt% m-TiO₂ loading.

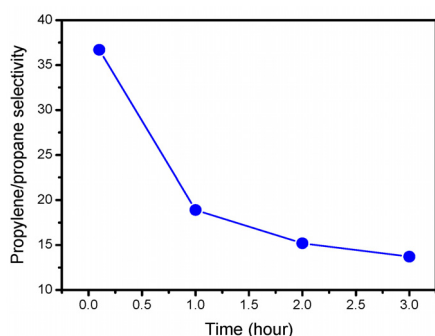


Fig. 4. Propylene/propane selectivity versus time of PVP/AgNP/TCNQ membranes with 10 wt% m-TiO₂ loading.

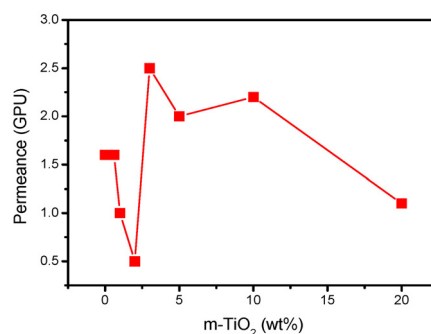


Fig. 5. Mixed-gas permeances of PVP/AgNP/TCNQ membranes with various m-TiO₂ loadings.

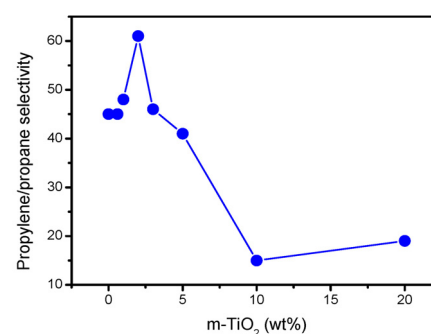


Fig. 6. Propylene/propane mixed-gas selectivities of PVP/AgNP/TCNQ membranes with various m-TiO₂ loadings.

composite were not positively polarized because of the absence of an electron acceptor such as TCNQ. On the other hand, when TCNQ was incorporated into the PVP/AgNP/TCNQ composite, the resulting membrane had the much greater propylene/propane selectivity of 45, and an increased mixed-gas permeance of 1.6 GPU. The increased selectivity was attributable to the positive polarized surface of the AgNPs, which was induced by the electron-accepting agent TCNQ. Thus, the positively polarized AgNPs could interact reversibly with propylene gas, thereby facilitating propylene transport and increasing the selectivity of propylene diffusion over propane diffusion.

The initial separation performance of PVP/AgNP/TCNQ/m-TiO₂ composite membranes was excellent. For example, the membrane with 10 wt% loading of m-TiO₂ showed mixed-gas permeance of 16.0 GPU and propylene/propane selectivity of 37 (Table 1). However, both permeance and selectivity decreased

considerably with time (Figs. 3 and 4); after 3 h, the permeance and selectivity respectively declined to 1.2 and 14. The reason for this is not presently clear, but we believe it might be related to a specific interaction between Ti and Ag[42,43] that causes the AgNPs to lose activity as olefin carriers. The mixed-gas permeance and propylene/propane selectivity through PVP/AgNP/TCNQ membranes of various m-TiO₂ content were measured during 3 h of permeation; the results are respectively shown in Figs. 5 and 6 versus m-TiO₂ content. The gas permeance decreased with increasing m-TiO₂ content up to 2 wt%, peaked at 2.5 GPU for the m-TiO₂ content of 3 wt%, and then gradually decreased with further increases in m-TiO₂ content. The enhanced permeance was presumably caused by facile mass transport through m-TiO₂ mesopores. However, the selectivity greatly decreased for m-TiO₂ loadings above 5 wt%, possibly owing to interfacial defects among the components.

4. Conclusions

In this study, m-TiO₂ was used as an agent to promote the formation of mass transport channels through facilitated olefin transport membranes consisting of PVP/AgNP/TCNQ. m-TiO₂ with anatase/rutile mixture phase and a crystallite size of 16 nm was fabricated by templating, using amphiphilic PVC-g-POEM graft copolymer as a structure-directing agent. The incorporation of the electron-accepting agent TCNQ greatly increased the mixed-gas permeance from 0.8 to 1.6 GPU and the propylene/propane selectivity from 1.1 to 45, owing to its effect of positively polarizing the surface of the AgNPs. The addition of m-TiO₂ led to a significant improvement in mixed-gas permeance, from 1.6 to 16.0 GPU, by facilitating mass transport through the mesopores. However, both the mixed-gas permeance and propylene/propane selectivity of PVP/AgNP/TCNQ/m-TiO₂ membranes gradually decreased with time, which might be attributed to specific interaction between TiO₂ and Ag NPs causing the Ag to lose activity as an olefin carrier. The use of non-interacting mesoporous metal oxide such as silica (SiO₂) would be effective in improving the facilitated olefin transport, which will be investigated in the near future.

Acknowledgements

We acknowledge financial support from the Active Polymer Center for Pattern Integration (2007-0056091), and the Energy Efficiency & Resources R&D program of the Korea Institute of Energy Technology Evaluation and Planning (KETEP)(20122010100040).

Reference

1. C. Zhu, S. Guo, Y. Zhai, and S. Dong, "Layer-by-layer self-assembly for constructing a graphene/platinum nanoparticle three-dimensional hybrid nanostructure using ionic liquid as a linker", *Langmuir*, **26**, 7614 (2010).
2. D. Li, Y. Cui, K. Wang, Q. He, X. Yan, and J. Li, "Thermosensitive nanostructures comprising gold nanoparticles grafted with block copolymers", *Adv. Funct. Mater.*, **17**, 3134 (2007).
3. C. Jiang, S. Markutsya, Y. Pikus, and V. V. Tsukruk, "Freely suspended nanocomposite membranes as highly sensitive sensors", *Nat. Mater.*, **3**, 721 (2004).
4. B.-S. Kim, J.-M. Qiu, J.-P. Wang, and T. A. Taton, "Magnetomicelles: composite nanostructures from magnetic nanoparticles and cross-linked amphiphilic block copolymers", *Nano Lett.*, **5**, 1987 (2005).
5. Y. Ding, M. Chen, and J. Erlebacher, "Metallic mesoporous nanocomposites for electrocatalysis", *J. Am. Chem. Soc.*, **126**, 6876 (2004).
6. J. Geng, K. Li, K. Y. Pu, D. Ding, and B. Liu, "Conjugated polymer and gold nanoparticle co loaded plga nanocomposites with eccentric internal nanostructure for dual-modal targeted cellular imaging", *Small*, **8**, 2421 (2012).
7. V. Bagalkot, L. Zhang, E. Levy-Nissenbaum, S. Jon, P. W. Kantoff, R. Langer, and O. C. Farokhzad, "Quantum dot-aptamer conjugates for synchronous cancer imaging, therapy, and sensing of drug delivery based on bi-fluorescence resonance energy transfer", *Nano Lett.*, **7**, 3065 (2007).
8. I. I. Slowing, B. G. Trewyn, S. Giri, and V. Y. Lin, "Mesoporous silica nanoparticles for drug delivery and biosensing applications", *Adv. Funct. Mater.*, **17**, 1225 (2007).
9. W. J. Rieter, K. M. Pott, K. M. Taylor, and W. Lin, "Nanoscale coordination polymers for platinum-based anticancer drug delivery", *J. Am. Chem. Soc.*, **130**, 11584 (2008).
10. B. G. Trewyn, S. Giri, I. I. Slowing, and V. S.-Y. Lin, "Mesoporous silica nanoparticle based controlled release, drug delivery, and biosensor systems", *Chem. Commun.*, 3236 (2007).
11. M. Delcea, H. Möhwald, and A. G. Skirtach, "Stimuli-responsive LbL capsules and nanoshells for drug delivery", *Adv. Drug Delivery Rev.*, **63**,

- 730 (2011).
12. D. Astruc, E. Boisselier, and C. Ornelas, "Dendrimers designed for functions: from physical, photophysical, and supramolecular properties to applications in sensing, catalysis, molecular electronics, photonics, and nanomedicine", *Chem. Rev.*, **110**, 1857 (2010).
 13. R. Singh and N. Zheludev, "Materials: Superconductor photonics", *Nat. Photonics*, **8**, 679 (2014).
 14. Y. Teow, A. Ahmad, J. Lim, and B. Ooi, "Preparation and characterization of PVDF/TiO₂ mixed matrix membrane via in situ colloidal precipitation method", *Desalination*, **295**, 61 (2012).
 15. S. Jessie Lue, J. Y. Chen, and J. Ming Yang, "Crystallinity and stability of poly (vinyl alcohol)-fumed silica mixed matrix membranes", *J. Macromol. Sci. Part B Phys.*, **47**, 39 (2007).
 16. L. Y. Ng, A. W. Mohammad, C. P. Leo, and N. Hilal, "Polymeric membranes incorporated with metal/metal oxide nanoparticles: a comprehensive review", *Desalination*, **308**, 15 (2013).
 17. T. B. Kang and S. R. Hong, "Separation of Hydrogen-Nitrogen Gases by PDMS-NaA zeolite Mixed Matrix Membranes", *Membr. J.*, **25**, 295 (2015).
 18. J. Ahn, W.-J. Chung, I. Pinnau, J. Song, N. Du, G. P. Robertson, and M. D. Guiver, "Gas transport behavior of mixed-matrix membranes composed of silica nanoparticles in a polymer of intrinsic microporosity (PIM-1)", *J. Membr. Sci.*, **346**, 280 (2010).
 19. C. Zhang, Y. Dai, J. R. Johnson, O. Karvan, and W. J. Koros, "High performance ZIF-8/6FDA-DAM mixed matrix membrane for propylene/propane separations", *J. Membr. Sci.*, **389**, 34 (2012).
 20. Y. I. Park, H. R. Song, S. E. Nam, Y. K. Hwang, J. S. Chang, and U. H. Lee, "Preparation and characterization of mixed-matrix membranes containing MIL-100(Fe) for gas separation", *Membr. J.*, **23**, 432 (2013).
 21. S. W. Kang, K. Char, and Y. S. Kang, "Novel application of partially positively charged silver nanoparticles for facilitated transport in olefin/paraffin separation membranes", *Chem. Mater.*, **20**, 1308 (2008).
 22. Y. S. Kang, S. W. Kang, H. Kim, J. H. Kim, J. Won, C. K. Kim, and K. Char, "Interaction with olefins of the partially polarized surface of silver nanoparticles activated by p-benzoquinone and its implications for facilitated olefin transport", *Adv. Mater.*, **19**, 475 (2007).
 23. I. S. Chae, S. W. Kang, J. Y. Park, Y. G. Lee, J. H. Lee, J. Won, and Y. S. Kang, "Surface Energy-level tuning of silver nanoparticles for facilitated olefin transport", *Angew. Chem. Int. Ed.*, **123**, 3038 (2011).
 24. M. Zhou, D. Korelskiy, P. Ye, M. Grahn, and J. Hedlund, "A uniformly oriented MFI membrane for improved CO₂ separation", *Angew. Chem. Int. Ed.*, **53**, 3492 (2014).
 25. E. H. Cho, K. B. Kim, and J. W. Rhim, "Transport properties of PEBAX blended membranes with peg and glutaraldehyde for SO₂ and other gases", *Polymer(KOREA)*, **38**, 687 (2014).
 26. D.-H. Kim, H.-S. Im, M.-S. Kim, B.-S. Lee, B.-S. Lee, S.-W. Yoon, B.-S. Kim, Y.-I. Park, S.-I. Cheong, and J.-W. Rhim, "Study on the gas permeation behaviors of surface fluorinated polysulfone membranes", *Polymer(KOREA)*, **33**, 537 (2009).
 27. L. M. Robeson, "The upper bound revisited", *J. Membr. Sci.*, **320**, 390-400 (2008).
 28. T. Zhou, L. Luo, S. Hu, S. Wang, R. Zhang, H. Wu, Z. Jiang, B. Wang, and J. Yang, "Janus composite nanoparticle-incorporated mixed matrix membranes for CO₂ separation", *J. Membr. Sci.*, **489**, 1 (2015).
 29. J. W. Rhim, C. S. Lee, E. H. Cho, S. Y. Ha, and J. T. Chung, "Multi-stage Process study of pei-pdms hollow fiber composite membrane modules for H₂/CO₂ mixed gas separation", *Membr. J.*, **23**, 1 (2013).
 30. Y. Kong, H. Du, J. Yang, D. Shi, Y. Wang, Y. Zhang, and W. Xin, "Study on polyimide/TiO₂ nanocomposite membranes for gas separation",

- Desalination*, **146**, 49 (2002).
31. S. Matteucci, V. A. Kusuma, D. Sanders, S. Swinnea, and B. D. Freeman, "Gas transport in TiO₂ nanoparticle-filled poly(1-trimethylsilyl-1-propyne)", *J. Membr. Sci.*, **307**, 196 (2008).
 32. F. Moghadam, M. R. Omidkhah, E. Vashghani-Farahani, M. Z. Pedram, and F. Dorosti, "The effect of TiO₂ nanoparticles on gas transport properties of Matrimid5218-based mixed matrix membranes", *Sep. Purif. Technol.*, **77**, 128 (2011).
 33. T. Yang and T. S. Chung, "High performance ZIF-8/PBI nano-composite membranes for high temperature hydrogen separation consisting of carbon monoxide and water vapor", *Int. J. Hydrogen Energy*, **38**, 229 (2013).
 34. H. Y. Zhao, Z. Jin, H. M. Su, J. L. Zhang, X. D. Yao, H. J. Zhao, and G. S. Zhu, "Target synthesis of a novel porous aromatic framework and its highly selective separation of CO₂/CH₄", *Chem. Commun.*, **49**, 2780 (2013).
 35. T.-S. Chung, L. Y. Jiang, Y. Li, and S. Kulprathipanja, "Mixed matrix membranes (MMMs) comprising organic polymers with dispersed inorganic fillers for gas separation", *Prog. Polym. Sci.*, **32**, 483 (2007).
 36. P. Burmann, B. Zornoza, C. Téllez, and J. Coronas, "Mixed matrix membranes comprising MOFs and porous silicate fillers prepared via spin coating for gas separation", *Chem. Eng. Sci.*, **107**, 66 (2014).
 37. D. K. Roh, S. J. Kim, W. S. Chi, J. K. Kim, and J. H. Kim, "Dual-functionalized mesoporous TiO₂ hollow nanospheres for improved CO₂ separation membranes", *Chem. Commun.*, **50**, 5717 (2014).
 38. S. H. Ahn, D. J. Kim, W. S. Chi, and J. H. Kim, "Hierarchical double-shell nanostructures of TiO₂ nanosheets on SnO₂ hollow spheres for high-efficiency, solid-state, dye-sensitized solar cells", *Adv. Func. Mater.*, **24**, 5037 (2014).
 39. S. H. Ahn, D. J. Kim, W. S. Chi, and J. H. Kim, "One-dimensional hierarchical nanostructures of TiO₂ nanosheets on SnO₂ nanotubes for high efficiency solid-state dye-sensitized solar cells", *Adv. Mater.*, **25**, 4893 (2013).
 40. W. S. Chi, S. J. Kim, S. J. Lee, Y. S. Bae, and J. H. Kim, "Enhanced performance of mixed-matrix membranes through a graft copolymer-directed interface and interaction tuning approach", *Chem. Sus. Chem.*, **8**, 650 (2015).
 41. G. H. Hong, D. Song, I. S. Chae, J. H. Oh, and S. W. Kang, "Highly permeable poly (ethylene oxide) with silver nanoparticles for facilitated olefin transport", *RSC Adv.*, **4**, 4905 (2014).
 42. T. Hirakawa and P. V. Kamat, "Charge separation and catalytic activity of Ag@ TiO₂ core-shell composite clusters under UV-irradiation", *J. Am. Chem. Soc.*, **127**, 3928 (2005).
 43. I. Pastoriza-Santos, D. S. Koktysh, A. A. Mamedov, M. Giersig, N. A. Kotov, and L. M. Liz-Marzán, "One-pot synthesis of Ag@ TiO₂ core-shell nanoparticles and their layer-by-layer assembly", *Langmuir*, **16**, 2731 (2000).